NF-κB Inhibition through Proteasome Inhibition or IKKβ Blockade Increases the Susceptibility of Melanoma Cells to Cytostatic Treatment through Distinct Pathways

Katharina Amschler[1,2,3,5], Michael P. Schön[1,2,3,5], Nadin Pletz[1], Katrin Wallbrecht[1], Luise Erpenbeck[1] and Margarete Schön[4]

Metastasized melanoma is almost universally resistant to chemotherapy. Given that constitutive or drug-induced upregulation of NF-κB activity is associated with this chemoresistance, NF-κB inhibition may increase the susceptibility to antitumoral therapy. On the cellular level, two principles of NF-κB inhibition, proteasome inhibition by bortezomib and IκB kinase-β (IKKβ) inhibition by the kinase inhibitor of NF-κB-1 (KINK-1), significantly increased the antitumoral efficacy of camptothecin. When combined with camptothecin, either of the two NF-κB-inhibiting principles synergistically influenced progression-related *in vitro* functions, including cell growth, apoptosis, and invasion through an artificial basement membrane. In addition, when C57BL/6 mice were intravenously injected with B16F10 melanoma cells, the combination of cytostatic treatment with either of the NF-κB-inhibiting compounds revealed significantly reduced pulmonary metastasis compared to either treatment alone. However, on the molecular level, nuclear translocation of p65, cell cycle analysis, and expression of NF-κB-dependent gene products disclosed distinctly different molecular mechanisms, resulting in the same functional effect. That proteasome inhibition and IKKβ inhibition affect distinct molecular pathways downstream of NF-κB, both leading to increased chemosensitivity, is previously unreported. Thus, it is conceivable that switching the two principles of NF-κB inhibition, once resistance to one of the agents occurs, will improve future treatment regimens.

Journal of Investigative Dermatology (2010) **130,** 1073–1086; doi:10.1038/jid.2009.365; published online 26 November 2009

INTRODUCTION

One of the central challenges of today's cancer management is intrinsic or acquired resistance of advanced tumors to antitumoral therapy (Wang *et al.*, 1999; Nakanishi and Toi, 2005). Melanoma, an aggressive skin cancer with the highest mortality of all skin diseases, vividly highlights this problem, as it is almost universally resistant to chemotherapy. Response rates to dacarbazine, the only agent approved by the Food and Drug Administration (FDA) for the treatment of metastatic melanoma, rarely exceed 5–10% (Helmbach *et al.*, 2001; Soengas and Lowe, 2003). In addition, numerous phase-III clinical trials, including antitumoral vaccination with or without dendritic cells, antibody- or cytokine-based immunotherapy, radiation, and chemotherapy, have yielded largely sobering results (Grossman *et al.*, 2001; Lens, 2008). It is thought that melanoma cells have acquired several mutually enhancing mechanisms, such as multidrug elimination or apoptosis deficiency, which lead to resistance against virtually all of the currently available therapeutic approaches (Grossman and Altieri, 2001; Soengas and Lowe, 2003).

Strategies employed by malignant tumors to evade antitumoral therapies include upregulation of the central transcription factor NF-κB that, among its function as a pivotal regulator of many cellular functions, contributes to aggressive growth and chemoresistance of some tumors (Kim *et al.*, 2006; Ueda and Richmond, 2006). The NF-κB family comprises five members: p50/p105 (NF-κB1), p52/p100 (NF-κB2), c-Rel, RelB, and p65 (RelA). Each of these protein subunits possesses a Rel-homology domain that is involved in DNA binding, dimerization, and interaction with IκB proteins (Karin and Lin, 2002; Kumar *et al.*, 2004; Perkins, 2007). In normal cells, NF-κB is retained in the cytoplasm through

[1]*Department of Dermatology and Venereology, Georg August University, Göttingen, Germany;* [2]*Rudolf Virchow Center, DFG Research Center for Experimental Biomedicine, Julius Maximilians University, Würzburg, Germany;* [3]*Department of Dermatology, Julius Maximilians University, Würzburg, Germany and* [4]*Department of Cellular and Molecular Immunology, Georg August University, Göttingen, Germany*

[5]*These authors contributed equally to this work.*

Correspondence: Michael P. Schön, Department of Dermatology and Venereology, Georg August University, Von-Siebold-Str. 3, Göttingen 37075, Germany. E-mail: michael.schoen@med.uni-goettingen.de

Abbreviations: GFP, green fluorescent protein; IKKβ, IκB kinase; KINK-1, kinase inhibitor of NF-κB-1; PBS, phosphate-buffered saline

Received 25 February 2009; revised 1 September 2009; accepted 13 September 2009; published online 26 November 2009

binding to inhibitory IκB proteins (IκBα, IκBβ, IκBγ). Stimulation of the IκB kinase (IKK) complex, for example, by tumor necrosis factor-α, lipopolysaccharide, IL-1, or other stimuli, leads to phosphorylation of IκB and, consecutively, release of NF-κB (Karin *et al.*, 2004). The latter can then translocate into the nucleus and initiate the transcription of cancer progression-relevant proteins such cytokines, chemokines, cyclin D1, matrix metalloproteinases, and antiapoptotic proteins (Baldwin, 2001; Yang and Richmond, 2001; Karin *et al.*, 2004; Karin, 2006). Upregulation of these proteins could mediate, at least in part, resistance to antitumoral treatments. In addition, some cytostatic compounds including doxorubicin (and other anthracycline drugs) or camptothecin activate NF-κB, thus presumably contributing themselves to chemoresistance of some cancer cells (Huang *et al.*, 2000). Therefore, the combinatorial treatment of tumors using NF-κB inhibition and chemotherapy is an intensively studied principle that has been tested in hematological malignancies and also in solid tumors such as colon cancer and melanoma (Arlt *et al.*, 2003; Amiri *et al.*, 2004; Fukuyama *et al.*, 2007; Schön *et al.*, 2008).

In fact, the proteasome inhibitor bortezomib, whose predominant biological effect is inhibition of NF-κB activation and, consecutively, downmodulation of NF-κB-dependent gene products, has been approved for the treatment of multiple myeloma and mantle cell lymphoma (Denz *et al.*, 2006). However, bortezomib exerts a number of off-target effects, thus showing a somewhat pleiotropic mode of action (Ciechanover and Schwartz, 1998; Paramore and Frantz, 2003; Chauhan *et al.*, 2005; Ludwig *et al.*, 2005; Nencioni *et al.*, 2006). Kinase inhibitor of NF-κB-1 (KINK-1) is a recently described highly selective small-molecule inhibitor of IKKβ (Schön *et al.*, 2008).

We provide here to our knowledge previously unreported evidence for distinctly different molecular changes induced by either of the two NF-κB-inhibiting principles, both eventually resulting in similar effects on the cellular level, namely, the desired enhanced susceptibility of melanoma cells to antitumoral treatment. It is, therefore, conceivable that switching and/or combining different NF-κB-inhibiting agents in the course of therapy will keep tumor cells susceptible to antitumoral treatments.

RESULTS

Differential activation of NF-κB and expression of NF-κB-regulated gene products in melanoma cell lines

Constitutive activation of NF-κB has been described as a hallmark feature in several tumors, including prostate cancer, breast cancer, multiple myeloma, pancreatic cancer, and melanoma (Davis *et al.*, 2001; Yang and Richmond, 2001; Liptay *et al.*, 2003). In contrast to normal melanocytes, many melanoma cells show constitutive activation of NF-κB (Amiri and Richmond, 2005). However, given that expression and activation of NF-κB in these tumors may vary widely, we first analyzed NF-κB activation in eight different melanoma lines. As shown by electrophoretic mobility shift assays (which detect activated NF-κB within the nuclear fraction of the cells), the lines MMNH, MV3, and MeWo showed the highest constitutive NF-κB activity, whereas Brown, Lox, and A375 showed intermediate levels, and Mel-2a showed the lowest signal intensity (Figure 1a). Activation of NF-κB results in constitutive transcription and expression of several NF-κB-dependent gene products in melanoma cells (Schön *et al.*, 2008). When eight melanoma cell lines were exposed to tumor necrosis factor-α, a treatment that induces profound activation of NF-κB through stimulation of the IKK complex, phosphorylation of IκB, and consecutive release of NF-κB, a marked enhancement of NF-κB was seen in the cell lines MeWo, MMNH, and MV3. The cell lines Brown, A375, and Lox showed moderate induction of NF-κB activity, and the lines SK-Mel-23 and Mel-2a did not respond detectably to incubation with tumor necrosis factor-α (Figure 1a). As shown

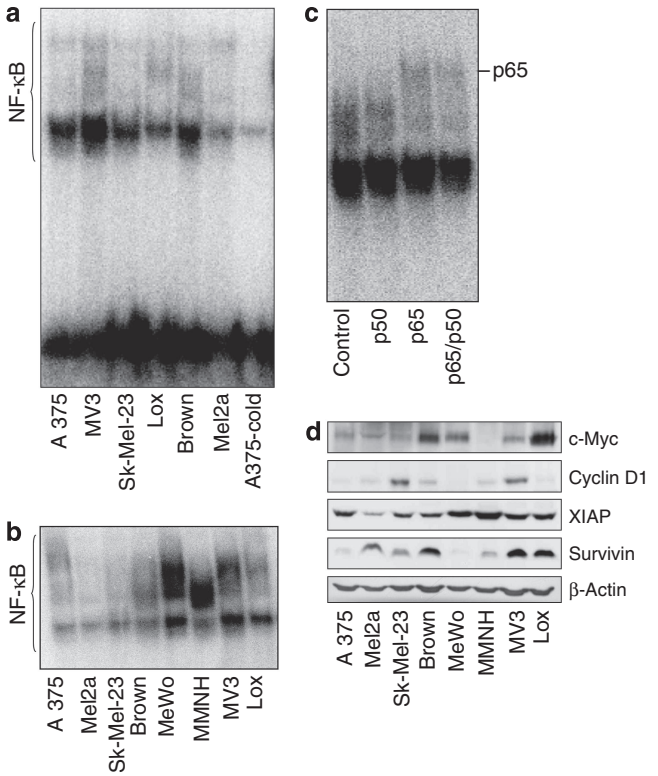

Figure 1. Differential activation of NF-κB and heterogeneous expression of NF-κB-dependent proteins in melanoma cells. (**a**) Constitutive NF-κB activation was assessed in six melanoma lines. Cells were lysed, nuclear extracts were prepared, and activated NF-κB was determined by electrophoretic mobility shift assays (EMSA) as outlined in Materials and Methods. The panel depicts an additional control lane (A375-cold) in which the specific signal was abrogated by unlabeled (cold) oligonucleotides to show specificity. (**b**) Tumor necrosis factor-α (TNFα)-stimulated NF-κB activation in eight melanoma lines. (**c**) Nuclear extracts of A375 melanoma cells were incubated with antibodies directed against p65, p50, or a combination of both for 30 minutes. Thereafter, NF-κB was determined by EMSA showing that probes containing p65 shifted the signal of the upper band to higher molecular weight. (**d**) Expression of the NF-κB-dependent proteins, c-MYC and cyclin D1, was detected by western blot analysis in the nuclear extracts; survivin and X-linked inhibitor of apoptosis protein (XIAP) were detected in cytosolic extracts. The lower panel shows the housekeeping protein β-actin.

by supershift assays (performed to detect specific NF-κB subunits within the nuclear extracts), the detected bands contained the p65 subunit (Figure 1b depicts the melanoma line A375 as an example).

In the next series of experiments, we analyzed the eight melanoma lines regarding expression of several gene products whose regulation is known to depend on NF-κB and which are involved in tumor progression-relevant cellular functions, such as proliferation or apoptosis. Proteins investigated in these experiments included c-MYC and cyclin D1, both regulators of the cell cycle, as well as X-linked inhibitor of apoptosis protein (XIAP) and survivin, two inhibitors of apoptosis. Again, the expression of these proteins showed considerable variability between the melanoma lines, and apparently the expression levels did not correlate with the levels of constitutive NF-κB activation in the respective melanoma lines (Figure 1c). Thus, the molecular heterogeneity of the melanoma lines tested suggested that it is not trivial to define common mechanisms that may explain the role of constitutive NF-κB activation for the malignant potential of a given tumor cell.

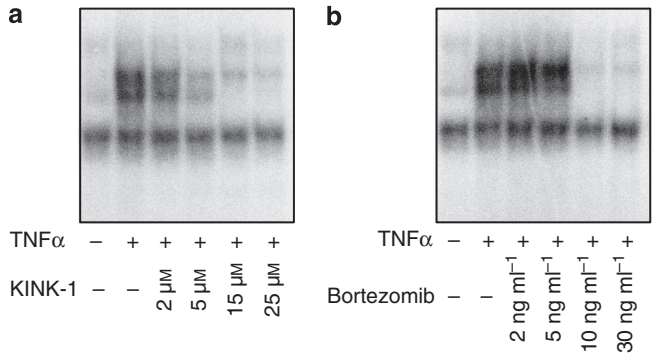

Figure 2. Bortezomib and kinase inhibitor of NF-κB-1 (KINK-1) inhibit activation and nuclear translocation of NF-κB. (**a**) Nuclear extracts were prepared from melanoma cells (cell line A375), which had been incubated with KINK-1 at the indicated concentrations for 18 hours. At 1 hour before harvesting, the medium was replaced by new medium containing tumor necrosis factor-α (TNFα) (1 nM) to stimulate activation and nuclear translocation of NF-κB. (**b**) NF-κB was detected by electrophoretic mobility shift assay in extracts from cells treated with bortezomib at the indicated concentrations for 18 hours. Again, activation and nuclear translocation of NF-κB was stimulated by TNFα (1 nM) 1 hour before harvesting.

Bortezomib and KINK-1 diminish NF-κB activity, but differentially affect NF-κB-dependent gene products

On the basis of its medium levels of constitutive NF-κB activation, inducibility of NF-κB activation, and average expression of several NF-κB-dependent gene products, the cell line A375 was primarily selected for further functional studies regarding the effects of NF-κB-inhibiting compounds *in vitro*. Most key findings were then confirmed with two other melanoma lines with similar characteristics, MMNH and MV3. Non-toxic doses (that is, doses which did not induce apoptosis or inhibition of cell proliferation) of KINK-1 and bortezomib were determined in a large series of dose–response experiments (data not shown). KINK-1 is a specific small-molecule inhibitor of IKKβ phosphorylation, an activity that was shown in three melanoma lines, MMNH, A375, and Mel-2a (Schön *et al.*, 2008). Given that recent reports suggested that bortezomib may actually upregulate NF-κB in some cancer cells (for example, endometrial carcinoma (Dolcet *et al.*, 2006)), we had to exclude first that NF-κB inhibitors exerted a similar ''paradoxical'' effect in melanoma cells. Therefore, the next series of experiments was designed to test the effect of both bortezomib and KINK-1 on NF-κB activity in melanoma cells. Electrophoretic mobility shift assays showed that the activity of NF-κB was decreased by both KINK-1 and bortezomib. While KINK-1 inhibited NF-κB activation in a clearly concentration-dependent manner (Figure 2a), bortezomib achieved rapid downregulation at high concentrations of $\geqslant 10\,\mathrm{ng\,ml^{-1}}$ (Figure 2b).

When NF-κB-regulated gene products implicated in tumor progression (Denkert *et al.*, 2001; Dhawan and Richmond, 2002; Payne and Cornelius, 2002; Eck *et al.*, 2003; Gazzaniga *et al.*, 2007) were studied under the influence of bortezomib or KINK-1, a clear-cut downregulation of the chemokines CXCL8 (IL-8), CXCL1 (Gro-α), and CCL1 (monocyte chemotactic protein-1 (MCP-1)) was found (Figure 3a). As shown by quantitative real-time PCR, this concentration-dependent downregulation of CXCL1 and CXCL8 was somewhat more pronounced when the melanoma cells were incubated with KINK-1 as compared with bortezomib. Although the concentration-dependent diminution of CCL1 (MCP-1) and CXCL8 (IL-8) correlated with diminished nuclear translocation of p65 (Figure 2), COX-2 (cyclooxygenase-2) expression appeared to increase again with higher KINK-1 concentrations (Figure 3a).

Some proteins involved in the regulation of apoptosis and/or cell proliferation (Levine, 1997; Oda *et al.*, 2000; Fernandez *et al.*, 2005) responded differentially when melanoma cells were exposed to bortezomib or KINK-1; although bortezomib induced a strong concentration-dependent upregulation of both NOXA and p53 (by 480 and 270%, respectively, as determined by densitometric analysis), this effect was not seen with KINK-1 (Figure 3b). In fact, NOXA was even downregulated by KINK-1 (by 40%). In contrast, bortezomib induced downregulation of cyclin D1 (by 50%) and, at high concentrations of $30\,\mathrm{ng\,ml^{-1}}$, led to decreased expression of survivin. The reduction of cyclin D1 was less pronounced when the cells were exposed to KINK-1, and expression of survivin was not affected by KINK-1. Expression of Bcl-X_L and the ratio of Bcl-2/Bax were not appreciably affected by either of the two compounds (Figure 3b).

Overall, bortezomib and KINK-1, both at concentrations sufficient to inhibit NF-κB activation, induced differential responses of some NF-κB-dependent gene products implicated in tumor progression, thus suggesting differences in their mode of action on the molecular level.

Differential cell cycle modulation in melanoma cells by bortezomib and KINK-1

Given that the expression of proteins involved in cell cycle regulation, such as cyclin D1 and p53, were differentially

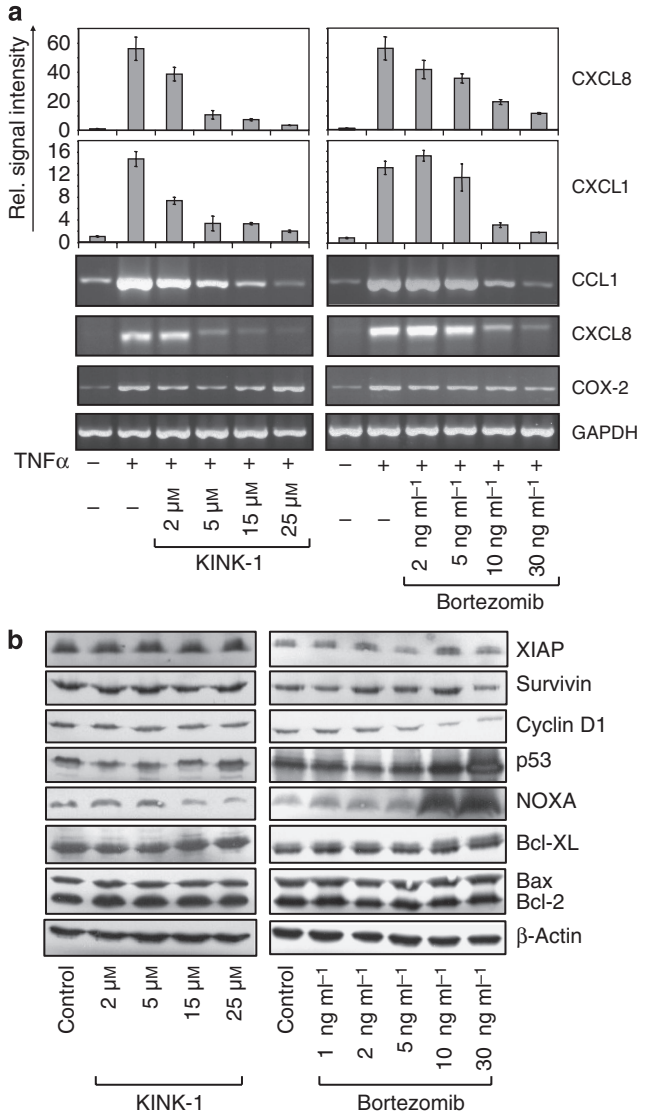

Figure 3. Differential response of NF-κB-regulated gene products to treatment with kinase inhibitor of NF-κB-1 (KINK-1) and bortezomib. (**a**) Melanoma cells (cell line A375) were exposed to KINK-1 or bortezomib at the indicated concentrations for 18 hours and stimulated with 1 nM tumor necrosis factor-α (TNFα). The upper four panels depict quantitative real-time PCR of mRNA expression of CXCL8 (IL-8) and CXCL1 (Gro-α). Values shown are the average of triplicate measurements (±SD), and the experiments were repeated twice with similar results. The lower panels depict semiquantitative reverse transcription-PCR results. (**b**) Melanoma cells were incubated with KINK-1 or bortezomib at the indicated concentrations for 18 hours. Several proteins involved in apoptosis and/or proliferation were detected by western blot analysis of nuclear extracts (cyclin D1 and p53), cytosolic extracts (X-linked inhibitor of apoptosis protein (XIAP) and survivin), or whole cell lysates (NOXA, Bcl-X_L, Bax, and Bcl-2) as outlined in Materials and Methods.

influenced by bortezomib and KINK-1, it was conceivable that the two compounds exerted divergent effects on the mitotic cycle of melanoma cells. To test this hypothesis, melanoma cells were exposed to KINK-1 (5 or 15 μM for 4 or 12 hours, respectively) or bortezomib (5 or 10 ng ml^{-1} for 4 or 12 hours, respectively) after thymidine treatment, a method that leads to an initial G1/S-phase arrest and subsequent ''synchronization'' of the cells. At 4 hours after being ''released'' by addition of fresh culture medium, all melanoma cell populations were predominantly in the G1/S-phase corresponding to the expected synchronizing effect of thymidine (Figure 4). However, remarkable differential effects of the two compounds became apparent after 12 hours: the majority of A375 cells treated with 5 μM KINK-1 reentered the mitotic cycle, and even in the population exposed to 15 μM KINK-1, only 56% of the cells were arrested in the G2/S-phase. In contrast, even low-dose treatment with bortezomib (5 ng ml^{-1}) led to long-lasting arrest of most cells (86%) in the G2/S-phase. Increasing the concentration of bortezomib to 10 ng ml^{-1} did not further enhance this effect (Figure 4). Thus, KINK-1 and bortezomib clearly showed differential effects on the cell cycle of melanoma cells.

Differential synergistic effects of KINK-1 and bortezomib with antitumoral treatment

To test the effect of the two NF-κB inhibitors on melanoma cells in the context of chemotherapeutic treatment, either of the two compounds (KINK-1 (5 μM), or bortezomib (5 ng ml^{-1})) was combined with camptothecin (0.03 μM, that is, a concentration that did not cause tumor cell apoptosis, as determined in dose–response experiments; data not shown). Both semiquantitative reverse transcription-PCR and quantitative real-time PCR (Figure 5a and b) determining several tumor progression-related gene products revealed some remarkable differences between the two NF-κB inhibitors: the camptothecin-induced chemokines, CXCL1 (Gro-α) and CXCL8 (IL-8), could both be repressed by KINK-1, whereas co-treatment with bortezomib did not reduce this activation (Figure 5a and b). In addition, CCL1 (MCP-1) was down-regulated by combinatorial treatment with camptothecin and KINK-1, but not with camptothecin and bortezomib (Figure 5a). In contrast, both the cdk inhibitor p21 and COX-2 were upregulated by camptothecin, but neither KINK-1 nor bortezomib antagonized this effect at non-toxic doses (Figure 5a).

When the induction of apoptosis in melanoma cells was studied, it was found that camptothecin-induced upregulation of the Bcl-2 family protein NOXA was markedly augmented by bortezomib, whereas KINK-1 achieved a less pronounced increase (Figure 5c). The ratio of Bcl-2 and Bax, an antiapoptotic and a pro-apoptotic protein of the Bcl-2 family (Figure 5c), or the expression of the inhibitors of apoptosis, XIAP and survivin (data not shown), were not detectably altered when suboptimal (that is, non-toxic) concentrations of camptothecin were combined with either KINK-1 or bortezomib. However, camptothecin stimulated the release of mitochondrial cytochrome C (a critical step in the mitochondrial pathway of apoptosis followed by binding to Apaf-1 and creation of the apoptosome). Bortezomib, but not KINK-1, led to a marked increase of the camptothecin-induced release of cytochrome C (Figure 5d).

As determined by the generation of histone-bound DNA fragments, both KINK-1 and bortezomib led to significantly increased apoptosis of melanoma cells to ~200% when

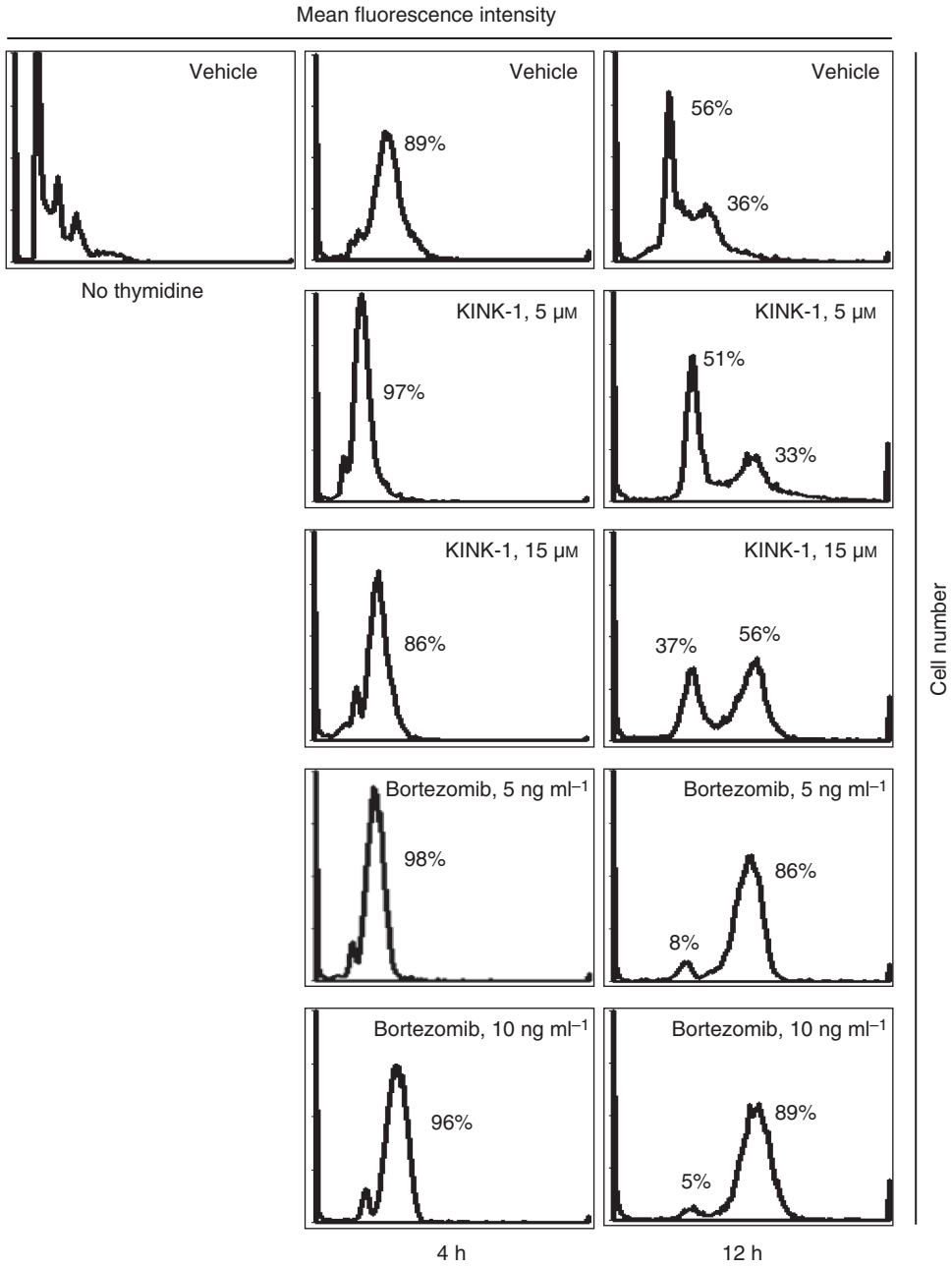

Figure 4. Differential effect of kinase inhibitor of NF-κB-1 (KINK-1) and bortezomib on the cell cycle of melanoma cells. Melanoma cells (cell line A375) were synchronized by thymidine treatment (2 mM) before incubation with vehicle, KINK-1 (5 or 15 μM), or bortezomib (5 or 10 ng ml^{-1}) for 4 hours or 12 hours, as indicated. Cell cycle analysis was performed after propidium iodide staining by flow cytometry, and the percentages of cells in the G1-phase (left peaks) and the G2-phase (right peaks) are shown. A control culture (upper left panel) was not synchronized by thymidine treatment.

combined with suboptimal concentrations of camptothecin (0.03 μM; $P<0.01$ and $P<0.05$, respectively, as compared with camptothecin alone; Figure 5e). When camptothecin was used at higher concentrations (0.10 μM), which were sufficient to kill melanoma cells, neither KINK-1 nor bortezomib increased the pro-apoptotic activity (Figure 5e). Thus, combinatorial treatment with either of the two NF-κB inhibitors increased the susceptibility of melanoma cells to treatment with camptothecin, although the molecular mechanisms underlying this synergistic effect appeared to differ between the two compounds.

Camptothecin-induced inhibition of melanoma cell invasion is potentiated by KINK-1 or bortezomib

Invasion through the extracellular matrix is a crucial step in tumor progression and NF-κB is a key regulator of gene products implicated in tumor cell invasion (for example, COX-2 and matrix metalloproteinase-9 (MMP-9)). On the basis of this notion, a two-well culture system was used to assess the invasion of fluorescently labeled melanoma cells into an artificial extracellular matrix in the presence of camptothecin, KINK-1, or bortezomib alone, as well as in the presence of camptothecin combined with KINK-1 or

bortezomib. As shown in Figure 6, camptothecin alone resulted in only moderate inhibition of melanoma cell invasion, and monotreatment with KINK-1 or bortezomib did not affect the invasive behavior of the cells. However, when suboptimal concentrations of camptothecin were combined with either of the NF-κB inhibitors, melanoma

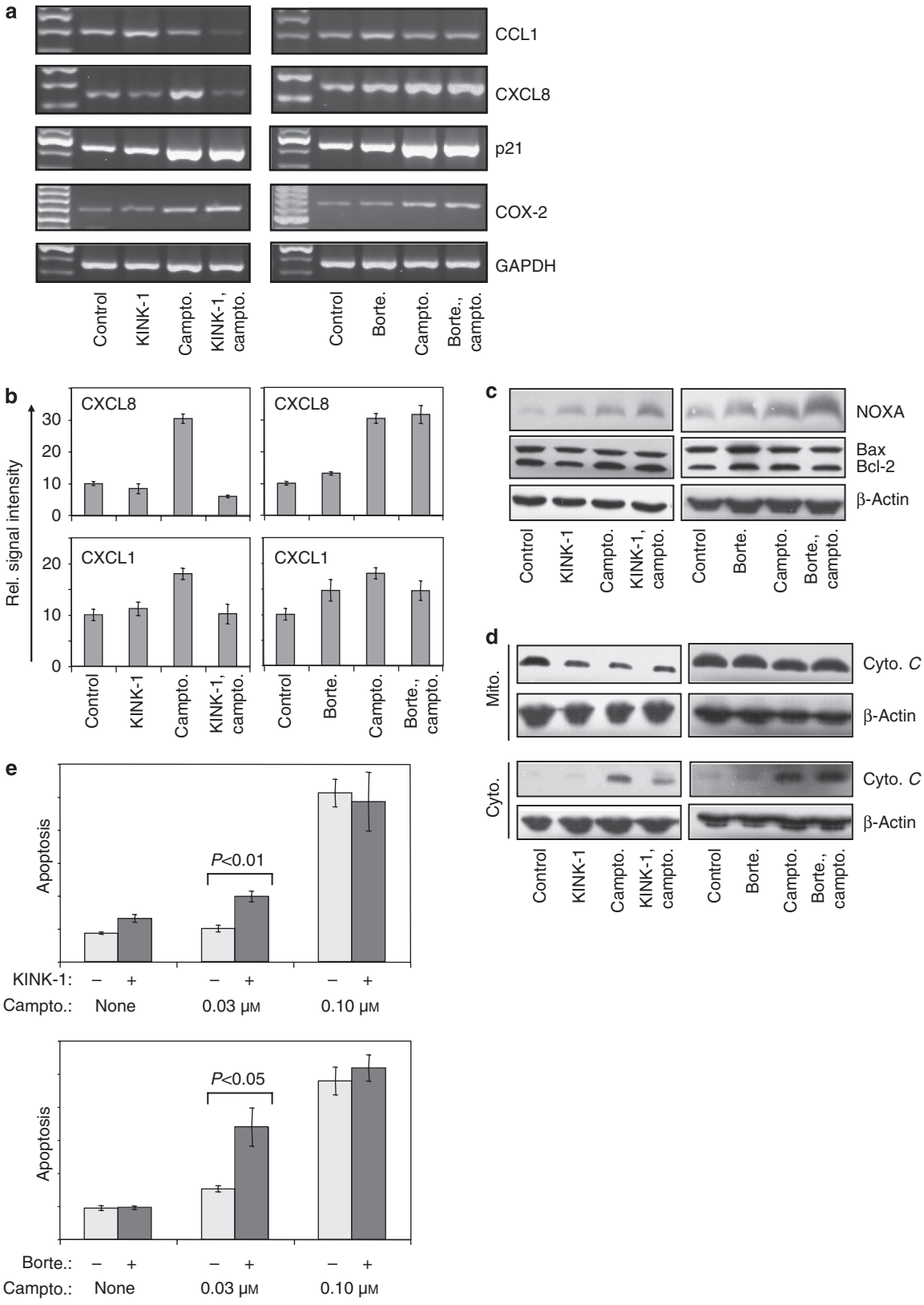

cell invasion was dramatically reduced. In particular, combination of camptothecin and KINK-1 resulted in complete abrogation of tumor cell invasion, whereas few invading cells were observed when camptothecin was combined with bortezomib (Figure 6).

Bortezomib and KINK-1 increase the antitumoral activity of camptothecin *in vivo*

To assess the *in vivo* efficacy of NF-κB inhibitors alone or in combination with camptothecin, a syngeneic system of C57BL/6 mice injected intravenously with B16F10 melanoma cells was used. Preliminary *in vitro* experiments had established that the murine melanoma cells showed similar apoptotic responses, inhibition of invasion, and regulation of several NF-κB-dependent gene products as the human A375 and MMNH melanoma lines when treated with camptothecin, KINK-1, bortezomib, or a combination thereof (data not shown). B16F10 melanoma cells (2.5×10^5 cells per mouse) were injected into the tail vein of C57BL/6 mice ($n = 6$ mice per group, the experiment was performed twice), and treatment was started 1 day after tumor cell injection. It had been established in another set of preliminary experiments using green fluorescent protein (GFP)-transfected B16F10 melanoma cells that intrapulmonary arrest of the tumor cells had taken place at this time point, thus excluding the possibility that the treatment interfered with the very early steps (for example, cell adhesion) of experimental metastasis (Figure 7a). When pulmonary metastasis in the experimental animals was evaluated 17 days after melanoma cell injection, it was found that multiple metastases had formed in the lungs of control mice as well as in the lungs of mice treated with either bortezomib ($0.5\,mg\,kg^{-1}$ on day 1 and 6, and $0.25\,mg\,kg^{-1}$ on day 11) or KINK-1 ($3\,mg\,kg^{-1}$ every other day; Figure 7b and c). Monotherapy with camptothecin ($1.8\,mg\,kg^{-1}$ every 3 days) resulted in moderate, not statistically significant reduction of pulmonary metastasis (Figure 7c). However, when the mice were treated by using a combination of camptothecin and bortezomib or KINK-1 a marked synergistic antitumoral response was evident. As determined by two objective methods, lung weight as a surrogate parameter for tumor masses (Figure 7c, upper panel) and computer-based morphometric analysis of metastasis-covered lung surfaces (Figure 7c, bottom panel), the combination of camptothecin with either of the two NF-κB inhibitors achieved significantly lower metastasis as compared with either therapy alone or the controls ($P < 0.01$ and $P < 0.05$, respectively).

To investigate the effects of camptothecin with and without the NF-κB inhibitors on cellular and molecular level *in vivo*, apoptosis in pulmonary melanoma metastases was assessed by TUNEL assays and apoptotic indices (percentage of TUNEL-positive cells within the tumor metastases) were calculated. It was found that monotherapy with either compound, camptothecin, bortezomib, or KINK-1, did not induce significant apoptosis in the melanoma metastases (apoptotic indices between 0.21 and 0.94) compared with untreated controls (apoptotic index 0.32; Figure 8a and b). In contrast, when mice were treated with a combination of camptothecin and bortezomib, the apoptotic index was 12.45 (SD = 3.28; $P < 0.001$ compared with either of the monotherapies; Figure 8a and b). Likewise, when mice were treated with a combination of camptothecin and KINK-1, the apoptotic index was 13.06 (SD = 3.79; $P < 0.001$ compared with either of the monotherapies; Figure 8a and b).

In metastases of untreated mice or mice treated by camptothecin monotherapy, nuclear expression of NF-κB could be detected in some tumor cells by immunohistochemistry. In contrast, such nuclear localization of NF-κB was not detectable in metastases of mice treated with bortezomib, KINK-1, or a combination of either of the NF-κB inhibitors with camptothecin, suggesting that nuclear NF-κB translocation has been inhibited *in vivo* (Figure 8c). Immunohistochemical staining of p53 and NOXA in the metastases did not reveal clear differences between the different mouse groups (data not shown).

DISCUSSION

Evidence for the involvement of NF-κB in oncogenesis is not new (Nakanishi and Toi, 2005). Indeed, many NF-κB-regulated gene products have been implicated in cellular transformation, proliferation, inhibition of apoptosis, invasion, angiogenesis, or metastasis (Karin *et al.*, 2002; Karin, 2006). On the one hand, many tumor cells, in contrast to their normal counterparts, show constitutive activation of NF-κB (Aggarwal, 2004; Kumar *et al.*, 2004; Karin, 2006). On the other hand, treatment of malignancies with some cytostatic compounds, such as anthracycline drugs or camptothecin, leads to induced activation of NF-κB (Huang *et al.*, 2000; Helmbach *et al.*, 2001; Laurent and Jaffrezou, 2001). The latter mechanism is considered a major cause for the development of inducible chemoresistance (Liu, 1989; Wang, 1996; Das and White, 1997; Wang *et al.*, 1999; Huang *et al.*, 2000; Laurent and Jaffrezou, 2001; Ivanov *et al.*, 2003). Thus, strategies to inhibit NF-κB in malignant tumors

Figure 5. Kinase inhibitor of NF-κB-1 (KINK-1) and bortezomib enhance the susceptibility of melanoma cells to cytostatic treatment with camptothecin. Melanoma cells (cell line A375) were incubated with vehicle (DMSO 0.1%, control), KINK-1 (5 μM), bortezomib (borte.) ($5\,ng\,ml^{-1}$), camptothecin (campto.) (0.03 μM), or combinations as indicated. (**a**) Expression of the indicated tumor progression-related NF-κB-regulated gene products was determined by semiquantitative reverse transcription-PCR. (**b**) CXCL8 and CXCL1 were assessed by quantitative real-time PCR. Values shown are the average of triplicate measurements (± SD), and the experiment was repeated twice with similar results. (**c**) Expression of the indicated apoptosis-related proteins was assessed by western blot analysis. (**d**) Cytochrome C (cyto. C) was determined by western blot analysis in the mitochondrial (mito.) and cytoplasmic (cyto.) fractions. The housekeeping protein β-actin is shown for each lysate. (**e**) Apoptosis was assessed in each of the cultures by determining the generation of histone-bound DNA fragments. Values shown are the average of triplicate measurements (± SD), and the experiment was repeated twice with similar results. The indicated *P*-values were determined using the two-tailed *t*-test.

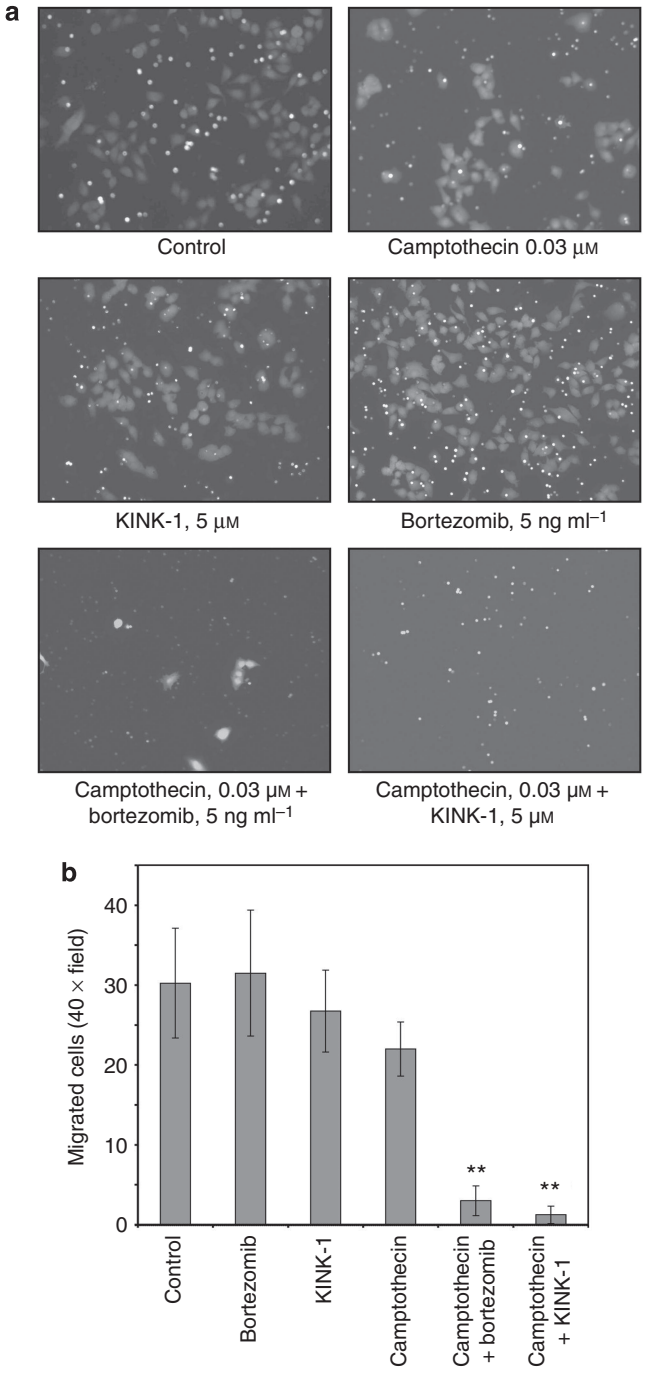

Figure 6. Inhibition of melanoma cell invasion by camptothecin is synergistically enhanced by kinase inhibitor of NF-κB-1 (KINK-1) or bortezomib. (**a**) Melanoma cells (cell line A375) were treated with the indicated concentrations of KINK-1, bortezomib, and camptothecin alone or in combination for 16 hours. The cells were then seeded into wells containing an artificial basement membrane and were allowed to invade this matrix for 24 hours. Fluorescent labeling of the cells was performed as outlined in Materials and Methods. The photomicrographs depict representative areas of each of the cultures. The cultures shown are representative of three independent experiments showing similar results. Bar = 20 μm (**b**) Quantitative analysis of three independent experiments. **Indicates $P = 0.00057$ for combinatorial treatment with camptothecin and bortezomib and $P = 0.00036$ for combinatorial treatment with camptothecin and KINK-1, respectively, as compared with the untreated control.

are considered a worthwhile addition to the current therapeutic armamentarium. The proteasome–ubiquitin system is currently the prime target for several pharmacological approaches, such as proteasome inhibitors, inhibitors of E1/E2 enzymes, inhibitors of E3 ubiquitin ligases, inhibitors of de-ubiquitinylating enzymes, or inhibitors of the proteasome–ubiquitin substrate surface (Guedat and Colland, 2007). The lead compound of the proteasome inhibitors, bortezomib, has been used in many clinical trials to treat various malignancies and is currently approved for the treatment of multiple myeloma and mantle cell lymphoma (Paramore and Frantz, 2003; Amiri *et al.*, 2004; Ludwig *et al.*, 2005; Denz *et al.*, 2006).

Nuclear factor-κB activation by camptothecin, a potent inhibitor of topoisomerase I that impairs DNA replication, RNA transcription, and DNA damage repair, involves degradation of IκB and depends on the presence of IKKβ, which are the two principles targeted in our study (Huang *et al.*, 2000). The efficacy of camptothecin in murine melanoma models has been shown previously (Liu, 1989; Dora *et al.*, 2006). In our experimental setting, NF-κB inhibition, either through proteasome inhibition by bortezomib (Huang *et al.*, 2000) or through IKKβ inhibition by the novel selective inhibitor KINK-1 (Schön *et al.*, 2008), led to significant synergistic enhancement of the antitumoral activity of camptothecin. When suboptimal concentrations of camptothecin were combined with either of the compounds, significant synergistic effects were observed regarding *in vitro* induction of melanoma cell apoptosis and suppression of invasion, as well as inhibition of *in vivo* metastasis in a murine model. However, the molecular mode of action of the two NF-κB inhibitors appeared to be conspicuously different. Although both strategies, IKKβ inhibition by KINK-1 and proteasome inhibition by bortezomib, showed the expected decrease of NF-κB activity, it is noteworthy that distinctly different regulations of some NF-κB-dependent gene products were observed (schematically depicted in Figure 9). Several hypotheses, which are not mutually exclusive, can be delineated to explain these observations at least in part.

First, proteasome inhibitors, such as bortezomib, may exert pleiotropic and/or off-target effects (Adams, 2004). Such effects include the dramatic upregulation of the pro-apoptotic protein NOXA, a salient feature of several proteasome inhibitors, as well as upregulation of p53, which were not seen with the IKKβ inhibitor, KINK-1. These effects are, at least in part, independent of proteasome inhibition or NF-κB inhibition (Nikiforov *et al.*, 2007). The net result would be that some gene products, which are not affected by more specific NF-κB inhibitors, are influenced by bortezomib. It is conceivable, of course, that KINK-1 also exerts off-target effects, but such an activity has not been shown yet, and it may be different from the effects exerted by bortezomib.

Second, the proteasome controls a plethora of survival factors in mammalian cells and it is involved in the degradation of all poly-ubiquitinylated proteins. Therefore, proteasome inhibition does not only lead to reduced

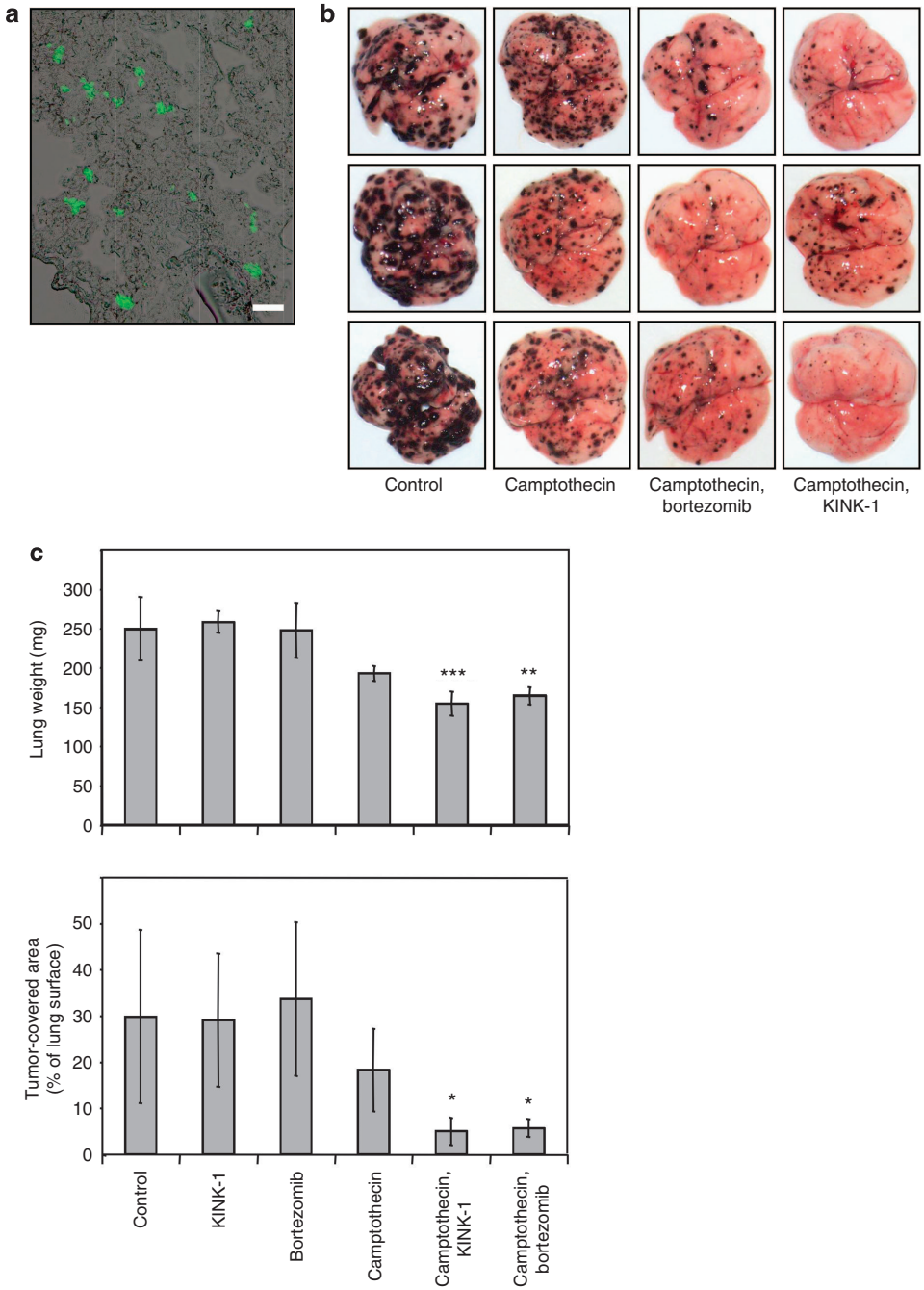

Figure 7. Kinase inhibitor of NF-κB-1 (KINK-1) and bortezomib enhance susceptibility of melanoma cells to camptothecin *in vivo*. (**a**) B16F10 melanoma cells were stably transfected with green fluorescent protein, and C57BL/6 mice were intravenously injected with 2.5×10^5 fluorescent cells per mouse. Cryostat-cut sections of the lungs of the animals were analyzed by fluorescence microscopy after 5 hours to visualize pulmonary arrest of the tumor cells. The photomicrograph shown is representative for similar results obtained with three mice. Bar = 50 μm. (**b**) Pulmonary metastasis was analyzed in C57BL/6 mice intravenously injected with 2.5×10^5 B16F10 melanoma cells and intraperitoneally treated with KINK-1, bortezomib, camptothecin, or combinations as indicated. Doses and treatment regimens were as outlined in the text. (**c**) Quantitative analysis of the antitumoral responses elicited by the indicated treatment regimens by two independent objective methods, lung weight as a surrogate parameter of tumor masses (upper panel) and computer-based analysis of tumor-covered lung surfaces (bottom panel). ***Indicates $P<0.001$, **indicates $P<0.01$, and *indicates $P<0.05$ compared with the effect of camptothecin alone. Comparison of combination treatments with treatment with the NF-κB inhibitors alone or with controls was always $P<0.001$.

degradation of IκB and, consecutively, reduced activity of NF-κB but also to alterations in a variety of other signaling molecules (Orlowski and Kuhn, 2008). It appears, therefore, that the proteasome inhibitor, bortezomib, exerts broader effects than the rather specific IKKβ inhibitor, KINK-1. However, whether these broader effects of bortezomib are generally beneficial or harmful in tumor therapy is not clear and may depend on the tumor type treated.

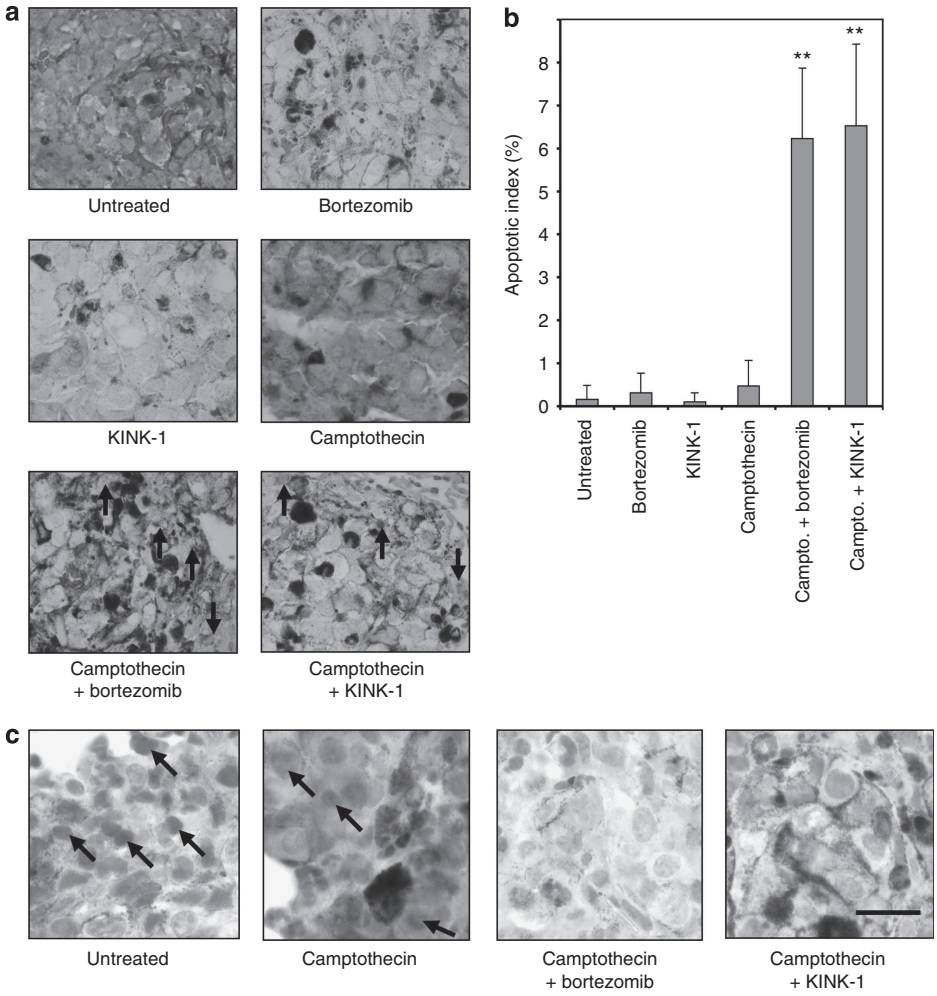

Figure 8. Synergistic effect of camptothecin and NF-κB inhibitors *in vivo*. (**a**) Pulmonary metastases were analyzed by a modified TUNEL assay in C57BL/6 mice intravenously injected with 2.5×10^5 B16F10 melanoma cells. Mice were either untreated or intraperitoneally treated with kinase inhibitor of NF-κB-1 (KINK-1), bortezomib, camptothecin, or combinations as indicated. Examples of TUNEL-positive nuclei (blue) are indicated by arrows. (**b**) Quantitative analysis of apoptotic cells in pulmonary melanoma metastases in C57BL/6 mice. Mice were treated as outlined in (**a**) and apoptotic cells were counted in at least five sections from each condition. The values shown represent the mean apoptotic index (± SD). **Indicates $P<0.001$. (**c**) NF-κB was detected by immunohistochemistry in pulmonary melanoma metastases of untreated mice or mice treated with camptothecin, or a combination of camptothecin and bortezomib or KINK-1 as indicated. Arrows highlight examples of tumor cells with nuclear detection of NF-κB. Bar = 20 μm.

Third, some gene products which are affected differently by proteasome inhibition or by IKKβ inhibition may be regulated redundantly by more than one transcription factor, thus evading the effect of a compound that specifically targets only NF-κB activation, such as KINK-1. Examples for such molecules are the E2F and the hypoxia-inducible factor-1α (HIF-1α) transcription factors, which are involved in the regulation of NOXA mRNA under stress (Hershko and Ginsberg, 2004; Kim *et al.*, 2004). Such gene products would respond to bortezomib, but not to KINK-1.

Fourth, expression of some NF-κB-regulated proteins including cyclin D1, survivin, and c-MYC did not correlate with translocation of p65 to the nucleus, a notion that is not easy to reconcile with the regulation of these genes by NF-κB. These observations underscore the complexity in the genetic response to NF-κB, thereby suggesting that posttranscriptional and posttranslational activation also participate in the expression of these proteins (Hassa and Hottiger, 1999; Campbell and Perkins, 2004). Although bortezomib-induced upregulation of NOXA has been attributed in part to regulation by c-MYC (Nikiforov *et al.*, 2007), the molecular mechanisms underlying upregulation of NOXA need to be clarified in further studies.

Fifth, bortezomib induced a longer-lasting and more profound cellular arrest as compared with KINK-1. It is, therefore, conceivable that the longer arrest of the cell cycle sensitizes bortezomib-treated tumor cells to low doses of camptothecin. In contrast, KINK-1 showed a less pronounced effect on the cell cycle, but it antagonized the camptothecin-induced upregulation of the tumor progression-related chemokines CCL1 (MCP-1), CXCL1 (Gro-α), and CXCL8 (IL-8) (Denkert *et al.*, 2001; Dhawan and Richmond, 2002;

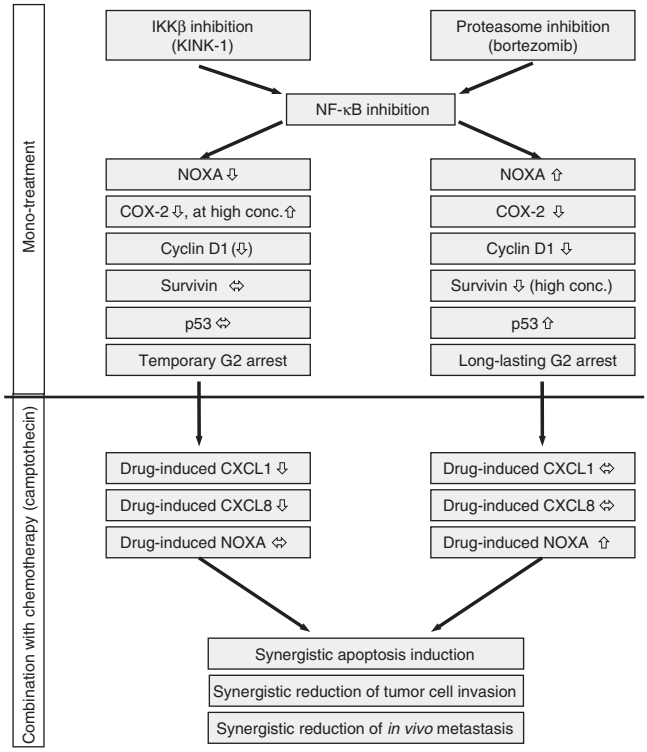

Figure 9. Bortezomib and KINK-1 enhance the susceptibility of melanoma cells to antitumoral treatment with camptothecin by different mechanisms. Schematic representation of putative modes of action of bortezomib and KINK-1 alone (upper part) and when combined with camptothecin (lower part). The figure summarizes some differences on the molecular level and similar net effects on the cellular level *in vitro* and *in vivo* as detailed in the text.

Payne and Cornelius, 2002; Eck *et al.*, 2003; Gazzaniga *et al.*, 2007; Koga *et al.*, 2008) more effectively as compared with bortezomib. The net effect, however, would be similar in both cases, that is, synergistic enhancement of the susceptibility of melanoma cells to antitumoral treatment by camptothecin.

Finally, NF-κB can be activated in a proteasome-independent fashion in some cells (Shumway and Miyamoto, 2004), a notion that suggests that other strategies of NF-κB inhibition, such as targeting IKKβ, may be more successful in such cells. Again, further studies are needed to determine whether melanoma cells possess the capacity to activate NF-κB in such a manner.

In any case, our results show that similar net effects achieved by different strategies of NF-κB inhibition, that is, profound synergistic reduction of melanoma cell invasion and metastasis when combined with a cytostatic drug, can be based on distinctly different molecular mechanisms (Figure 8). This notion may carry therapeutic implications in at least two ways: on the one hand, it is conceivable that switching NF-κB-inhibiting agents, once resistance to the first compound has occurred, will keep the tumor cells susceptible to antitumoral treatment. On the other hand, one might consider combining two (or more) NF-κB-inhibiting principles with distinct molecular modes of action, thus more effectively preventing the development of chemoresistance and reducing the risk of unwanted side effects. In addition, as bortezomib may induce *de novo* chemoresistance in some tumors (Chauhan *et al.*, 2004a, b; Kuhn *et al.*, 2007), combining this drug with another NF-κB-inhibiting drug may be advantageous. These hypotheses, however, need to be tested in further studies (Figure 9).

MATERIALS AND METHODS

Cells and culture conditions

Human melanoma lines A 375, Mel-2a, SK-Mel 23, Brown, MeWo, MMNH, MV3, and Lox and the murine melanoma line B16F10 were grown in DMEM supplemented with 10% fetal calf serum, 100 U ml^{-1} penicillin, and 100 μg ml^{-1} streptomycin (Gibco, Karlsruhe, Germany).

Western blot analysis

Protein concentrations in the cytoplasmic, mitochondrial, and nuclear fractions, as well as in whole cell lysates were determined by the Bradford assays. Equal amounts of protein were separated by SDS-PAGE and transferred onto nitrocellulose membranes. Proteins of interest were detected using mAb followed by peroxidase-labeled goat anti-mouse IgG or peroxidase-labeled goat anti-rabbit IgG and a chemiluminescence reaction (ECL, Amersham, Buckinghamshire, UK). Anti-human Bax (2D2; Biozol, Eching, Germany), anti-human Bcl-X_L (H-5; Santa Cruz Biotechnology, Heidelberg, Germany), anti-human survivin (D-8; Santa Cruz Biotechnology), anti-human p53 (Pab421, Calbiochem, San Diego, CA), and anti-human c-MYC (9E10; Santa Cruz Biotechnology) were used at 1:50 dilutions. Anti-human XIAP (2F1; Biozol), anti-human β-actin (Abcam, Biozol), and anti-human cyclin D1 (DCS6; Cell Signaling, Danvers, MA) were used at 1:1,000 dilutions. Anti-human cytochrome C (7H8.2C12; Becton Dickinson, Heidelberg, Germany), anti-human NOXA (114C307.1; Imgenex, San Diego, CA), and anti-human Bcl-2 (clone 124; DAKO Cytomation, Hamburg, Germany) were used at 1:500 dilutions.

Electrophoretic mobility shift assays

Subcellular fractionation and preparation of nuclear extracts was performed as described previously (Schön *et al.*, 2008). Equal amounts of protein (determined by Bradford assay) from nuclear extracts (10 μg) of cells treated with KINK-1 (2, 5, 15, or 25 μM), Bortezomib (2, 5, 10, or 30 ng ml^{-1}), and tumor necrosis factor-α (1 nM) were incubated with ^{32}P end-labeled, double stranded NF-κB oligonucleotide (5′-AGTTGAGGGGACTTTCCCAGGC-3′) (Gel shift assay systems; Promega, Madison, WI) for 20 minutes at room temperature. Subsequently, the DNA–protein complexes were resolved in a 6.6% native polyacrylamide gel. For supershift assays, nuclear extracts (10 μg) were incubated with antibodies (1 μg) against p65 (F-6), p50 (E-10; both from Santa Cruz Biotechnology) or a combination of both for 30 minutes at 20 °C before analysis by electrophoretic mobility shift assays. Radioactive signals were visualized and quantitated using a PhosphorImager and the Image Quant software (BioRad, Munich, Germany).

Semiquantitative reverse transcription-PCR

RNA from treated or untreated cells was extracted using the Rneasy Mini Kit (Qiagen, Hilden, Germany) according to the manufacturer's

instructions. Gene expression was assessed by reverse transcription-PCR (Oostingh *et al.*, 2007). Primers and reaction conditions are indicated in Supplementary Table S1.

Quantitative real-time PCR

cDNA was prepared from RNA of cells that were treated with either vehicle or with KINK-1, bortezomib, camptothecin, or combinations indicated in the text for 18 hours. PCR was performed according to the manual using the Quanti Tect Primer Assays (Qiagen) for human CXCL1, CXCL8, and glyceraldehyde-3-phosphate dehydrogenase (GAPDH). Each PCR was carried out in triplicate in a 25 µl volume using Quanti Tect SYBR Green Kits (Qiagen) for 5 minutes at 95 °C for initial denaturing, followed by 40 cycles of 95 °C for 10 seconds, and 60 °C for 30 seconds in the ABI Prism 7000 Sequence detection system. Values for each gene were normalized to the expression of GAPDH. Experiments were repeated twice.

Proliferation assay (3-(4,5-dimethylthiazol-2-yl)-5-(3-carboxymethoxyphenyl)-2-(4-sulfophenyl)-2H-tetrazolium (MTS)-assay)

Cells were plated at a density of 3,000 cells per well in a 96-well plate. Subconfluent cultures were treated with KINK-1, bortezomib, camptothecin, or combinations thereof as indicated in the text in a final volume of 100 µl. After 24 or 48 hours, the Cell Titer 96 Aq_{ueous} One Solution Cell Proliferation Assay (Promega, Mannheim, Germany) was used as described in the manual to measure proliferation of the cells.

Apoptosis detection (DNA fragmentation assay)

To assess apoptotic responses, cultured cells were incubated with apoptotic stimuli for 16 hours, lyzed and, by centrifugation at $10{,}000 \times g$ for 10 minutes, a clear supernatant was prepared. Equal amounts were added to microtiter plates coated with anti-histone antibodies, and incubated for 90 minutes at 20 °C. Histone-bound DNA fragments were detected using the Cell Death Detection ELISA according to the manual (Roche Diagnostics, Penzberg, Germany). The substrate reaction, resulting in a green color, was quantitated using an ELISA reader at 405 nm.

Thymidine treatment for G1/S-phase synchronization and cell cycle analysis

Subconfluent cell cultures were incubated with 2 mM thymidine for 16 hours, washed thrice with phosphate-buffered saline (PBS), and grown in DMEM containing 0.5% fetal calf serum for 10 hours. Thereafter, 2 mM thymidine was added for 14 hours. Cells were washed again thrice with PBS and then released with 10% fetal calf serum-containing medium (a treatment that initiates the cell cycle, thus ''synchronizing'' the cells) for 4 or 12 hours. Thymidine-treated cells as well as non-synchronized cells received either DMSO (0.1%, control), bortezomib (5 or 10 ng ml^{-1}), or KINK-1 (5 or 15 µM). For cell cycle analysis, the fixed cells (70% ethanol on ice) were washed thrice and resuspended in cold PBS containing 5 µg ml^{-1} propidium iodide and 0.1 mg ml^{-1} RNase A. Flow cytometry was performed using a FACS Calibur and the CellQuest software (BD, Heidelberg, Germany).

In vitro invasion assay

The invasiveness of melanoma cells was assayed in membrane invasion culture system by plating the cells on top of a matrigel-coated, fluorescence-blocking polycarbonate membrane with 8 µm pores (BD BioCoat Tumor Invasion System; Becton Dickinson). Melanoma cells were treated with bortezomib (5 ng ml^{-1}), KINK-1 (5 µM), camptothecin (0.03 µM), or combinations thereof for 16 hours, harvested by trypsin, and washed thrice with DMEM. Thereafter, the cells were seeded at a density of 5×10^4 cells per 500 µl DMEM on the matrigel-coated membrane in the upper compartment. The lower compartment was filled with 750 µl DMEM containing 10% fetal calf serum as a chemoattractant, and the plates were incubated at 37 °C for 24 hours. At the end of the incubation time, the insert plate was transferred into a second 24-well plate containing 0.5 ml per well of 4 µg ml^{-1} Calcein acetoxymethylester (Molecular Probes, Carlsbad, CA) in PBS (Gibco) and incubated for 1 hour at 37 °C to stain cells that invaded through the Matrigel. Finally, the fluorescence-labeled cells were quantitated using a fluorescence microscope (Axiovert 200, Zeiss, Göttingen, Germany).

Experimental pulmonary metastasis

Mouse experiments were approved by the appropriate authorities (Regierung von Unterfranken, Würzburg, Germany). Mice were housed in a climate-controlled specific pathogen-free facility and, at the time of termination of the experiment, were killed by ether anesthesia followed by cervical dislocation according to the institutional guidelines. C57BL/6 mice ($n = 6$ animals per group) were injected into the tail vein with 2.5×10^5 B16F10 murine melanoma cells. Treatment was started 1 day after melanoma cell injection. Treatment regimens were as follows: group 1—control: no treatment; group 2—KINK-1: 3 mg kg^{-1} every other day; group 3—bortezomib: 0.5 mg kg^{-1} on days 1 and 6, 0.25 mg kg^{-1} on day 11; group 4—camptothecin: 1.8 mg kg^{-1} on days 2, 5, 7, 10, 13, and 15; group 5—camptothecin and KINK-1: combination of both compounds using the same regimens as in the respective monotherapy groups; group 6—bortezomib and camptothecin: combination of both compounds using the same regimens as in the respective monotherapy groups. Metastasis was evaluated at day 17 after melanoma cell injection. Camptothecin was dissolved in PBS pH 7.4 containing 0.3% sodium carboxymethylcellulose and 0.2% Tween 80 as described (Dora *et al.*, 2006). All animal experiments were performed independently twice.

Apoptosis detection in pulmonary metastases by TUNEL assays

To prevent the loss of low-molecular-weight DNA fragments, lung specimens fixed in 4% paraformaldehyde were used for apoptosis detection. Paraffin-embedded sections were subjected to a modified TUNEL technique (DermaTACS) according to the manufacturer's recommendations (R&D Systems, Wiesbaden, Germany). In this assay, apoptotic cells are visualized by TACS Blue Label (R&D Systems) as blue nuclear staining in cells with DNA fragmentation. One section from each tissue block was incubated with TACS nuclease in order to generate DNA fragmentation in all cells (positive control). In another section, TdT was omitted (negative control). Apoptotic cells were quantitated microscopically in at least five metastases from each condition in a blinded fashion, and the apoptotic index was calculated as percentage of TUNEL-positive cells.

GFP transfection and short-term melanoma metastasis

B16F10 melanoma cells were stably transfected with GFP according to an optimized protocol for B16F10 using 1.5×10^6 cells, 2 µg of

pmaxGFP, and 100 μl of Nucleofactor solution V (Amaxa, Cologne, Germany). Transfected cells with high expression of GFP were sorted by flow cytometry, subcloned thrice, and cultured in DMEM medium (Gibco) containing 1 mg ml^{-1} of the G418 selection supplement (Sigma, Deisenhofen, Germany). GFP-expressing B16F10 melanoma cells (2.5×10^5) were injected into the tail vein of C57BL/6 mice ($n = 3$ animals per group) and killed after 5 hours to verify that pulmonary cell arrest had occurred before initiating antitumoral treatment. Cryostat-cut sections of the lung were assessed microscopically (Zeiss Axioskop). Overlays of phase contrast and fluorescence microscopy allowed precise topographic analysis of the tumor cells within the lung tissue.

Statistical analyses

Data are displayed as mean ± SD; *P*-values were determined using the two-tailed *t*-test and *P*-values < 0.05 (confidence interval of 95%) were considered statistically significant. All statistical tests were two-sided.

CONFLICT OF INTEREST

The authors state no conflict of interest.

ACKNOWLEDGMENTS

This work was supported by research grants from the Deutsche Krebshilfe to MS and MPS (10-2196 Schö-2), the Interdisciplinary Collaborative Research Center Würzburg to MS and MPS (project B42), and by a Rudolf Virchow Award from the Deutsche Forschungsgemeinschaft to MPS. The authors thank H. Sennefelder for excellent technical assistance.

SUPPLEMENTARY MATERIAL

Supplementary material is linked to the online version of the paper at http://www.nature.com/jid

REFERENCES

Adams J (2004) The proteasome: a suitable antineoplastic target. *Nat Rev Cancer* 4:349–60

Aggarwal BB (2004) Nuclear factor-kappaB: the enemy within. *Cancer Cell* 6:203–8

Amiri KI, Horton LW, LaFleur BJ *et al.* (2004) Augmenting chemosensitivity of malignant melanoma tumors via proteasome inhibition: implication for bortezomib (VELCADE, PS-341) as a therapeutic agent for malignant melanoma. *Cancer Res* 64:4912–8

Amiri KI, Richmond A (2005) Role of nuclear factor-κB in melanoma. *Cancer Metast Rev* 24:301–13

Arlt A, Gehrz A, Muerkoster S *et al.* (2003) Role of NF-kappaB and Akt/PI3K in the resistance of pancreatic carcinoma cell lines against gemcitabine-induced cell death. *Oncogene* 22:3243–51

Baldwin AS (2001) Control of oncogenesis and cancer therapy resistance by the transcription factor NF-kappaB. *J Clin Invest* 107:241–6

Campbell KJ, Perkins ND (2004) Post-translational modification of RelA(p65) NF-kappaB. *Biochem Soc Trans* 32:1087–9

Chauhan D, Hideshima T, Anderson KC (2005) Proteasome inhibition in multiple myeloma: therapeutic implication. *Annu Rev Pharmacol Toxicol* 45:465–76

Chauhan D, Li G, Podar K *et al.* (2004a) Targeting mitochondria to overcome conventional and bortezomib/proteasome inhibitor PS-341 resistance in multiple myeloma (MM) cells. *Blood* 104:2458–66

Chauhan D, Li G, Podar K *et al.* (2004b) The bortezomib/proteasome inhibitor PS-341 and triterpenoid CDDO-Im induce synergistic anti-multiple myeloma (MM) activity and overcome bortezomib resistance. *Blood* 103:3158–66

Ciechanover A, Schwartz AL (1998) The ubiquitin-proteasome pathway: the complexity and myriad functions of proteins death. *Proc Natl Acad Sci USA* 95:2727–30

Das KC, White CW (1997) Activation of NF-kappaB by antineoplastic agents. Role of protein kinase C. *J Biol Chem* 272:14914–20

Davis RE, Brown KD, Siebenlist U *et al.* (2001) Constitutive nuclear factor kappaB activity is required for survival of activated B cell-like diffuse large B cell lymphoma cells. *J Exp Med* 194:1861–74

Denkert C, Kobel M, Berger S *et al.* (2001) Expression of cyclooxygenase 2 in human malignant melanoma. *Cancer Res* 61:303–8

Denz U, Haas PS, Wäsch R *et al.* (2006) State of the art therapy in multiple myeloma and future perspectives. *Eur J Cancer* 42:1591–600

Dhawan P, Richmond A (2002) Role of CXCL1 in tumorigenesis of melanoma. *J Leukoc Biol* 72:9–18

Dolcet X, Llobet D, Encinas M *et al.* (2006) Proteasome inhibitors induce death but activate NF-kappaB on endometrial carcinoma cell lines and primary culture explants. *J Biol Chem* 281:22118–30

Dora CL, Alvarez-Silva M, Trentin AG *et al.* (2006) Evaluation of antimetastatic activity and systemic toxicity of camptothecin-loaded microspheres in mice injected with B16-F10 melanoma cells. *J Pharm Pharm Sci* 9:22–31

Eck M, Schmausser B, Scheller K *et al.* (2003) Pleiotropic effects of CXC chemokines in gastric carcinoma: differences in CXCL8 and CXCL1 expression between diffuse and intestinal types of gastric carcinoma. *Clin Exp Immunol* 134:508–15

Fernandez Y, Verhaegen M, Miller TP *et al.* (2005) Differential regulation of noxa in normal melanocytes and melanoma cells by proteasome inhibition: therapeutic implications. *Cancer Res* 65:6294–304

Fukuyama R, Ng KP, Cicek M *et al.* (2007) Role of IKK and oscillatory NFkappaB kinetics in MMP-9 gene expression and chemoresistance to 5-fluorouracil in RKO colorectal cancer cells. *Mol Carcinog* 46:402–13

Gazzaniga S, Bravo AI, Guglielmotti A *et al.* (2007) Targeting tumor-associated macrophages and inhibition of MCP-1 reduce angiogenesis and tumor growth in a human melanoma xenograft. *J Invest Dermatol* 127:2031–41

Grossman D, Altieri DC (2001) Drug resistance in melanoma: mechanisms, apoptosis, and new potential therapeutic targets. *Cancer Metastasis Rev* 20:3–11

Grossman D, Kim PJ, Schechner JS *et al.* (2001) Inhibition of melanoma tumor growth *in vivo* by survivin targeting. *Proc Natl Acad Sci USA* 98:635–40

Guedat P, Colland F (2007) Patented small molecule inhibitors in the ubiquitin proteasome system. *BMC Biochem* 8:1–12

Hassa PO, Hottiger MO (1999) A role of poly (ADP-ribose) polymerase in NF-kappaB transcriptional activation. *Biol Chem* 380:953–9

Helmbach H, Rossmann E, Kern MA *et al.* (2001) Drug-resistance in human melanoma. *Int J Cancer* 93:617–22

Hershko T, Ginsberg D (2004) Up-regulation of Bcl-2 homology 3 (BH3)-only proteins by E2F1 mediates apoptosis. *J Biol Chem* 279:8627–34

Huang TT, Wuerzberger-Davis SM, Seufzer BJ *et al.* (2000) NF-kappaB activation by camptothecin. A linkage between nuclear DNA damage and cytoplasmic signaling events. *J Biol Chem* 275:9501–9

Ivanov VN, Bhoumik A, Ronai Z (2003) Death receptors and melanoma resistance to apoptosis. *Oncogene* 22:3152–61

Karin M (2006) Nuclear factor-kappaB in cancer development and progression. *Nature* 441:431–6

Karin M, Cao Y, Greten FR *et al.* (2002) NF-kappaB in cancer: from innocent bystander to major culprit. *Nat Rev Cancer* 2:301–10

Karin M, Lin A (2002) NF-kappaB at the crossroads of life and death. *Nat Immunol* 3:221–7

Karin M, Yamamoto Y, Wang QM (2004) The IKK NF-kappa B system: a treasure trove for drug development. *Nat Rev Drug Discov* 3:17–26

Kim HJ, Hawke N, Baldwin AS (2006) NF-kappaB and IKK as therapeutic targets in cancer. *Cell Death Differ* 13:738–47

Kim JY, Ahn HJ, Ryu JH *et al.* (2004) BH3-only protein Noxa is a mediator of hypoxic cell death induced by hypoxia-inducible factor 1alpha. *J Exp Med* 199:113–24

Koga M, Kai H, Egami K *et al.* (2008) Mutant MCP-1 therapy inhibits tumor angiogenesis and growth of malignant melanoma in mice. *Biochem Biophys Res Commun* 365:279–84

Kuhn DJ, Chen Q, Voorhees PM *et al.* (2007) Potent activity of carfilzomib, a novel, irreversible inhibitor of the ubiquitin-proteasome pathway, against preclinical models of multiple myeloma. *Blood* 110:3281–90

Kumar A, Takada Y, Boriek AM *et al.* (2004) Nuclear factor-kappaB: its role in health and disease. *J Mol Med* 82:434–48

Laurent G, Jaffrezou JP (2001) Signaling pathways activated by daunorubicin. *Blood* 98:913–24

Lens M (2008) The role of vaccine therapy in the treatment of melanoma. *Expert Opin Biol Ther* 8:315–23

Levine AJ (1997) p53, the cellular gatekeeper for growth and division. *Cell* 88:323–31

Liptay S, Weber CK, Ludwig L *et al.* (2003) Mitogenic and antiapoptotic role of constitutive NF-kappaB/Rel activity in pancreatic cancer. *Int J Cancer* 105:735–46

Liu LF (1989) DNA topoisomerase poisons as antitumor drugs. *Annu Rev Biochem* 58:351–75

Ludwig H, Khayat D, Giaccone G *et al.* (2005) Proteasome inhibition and its clinical prospects in the treatment of hematologic and solid malignancies. *Cancer* 104:1794–807

Nakanishi C, Toi M (2005) Nuclear factor-kappaB inhibitors as sensitizers to anticancer drugs. *Nat Rev Cancer* 5:297–309

Nencioni A, Schwarzenberg K, Brauer KM *et al.* (2006) Proteasome inhibitor bortezomib modulates TLR4-induced dendritic cell activation. *Blood* 108:551–8

Nikiforov MA, Riblett M, Tang WH *et al.* (2007) Tumor cell-selective regulation of NOXA by c-MYC in response to proteasome inhibition. *Proc Natl Acad Sci USA* 104:19488–93

Oda E, Ohki R, Murasawa H *et al.* (2000) Noxa, a BH3-only member of the Bcl-2 family and candidate mediator of p53-induced apoptosis. *Science* 288:1053–8

Oostingh GJ, Schlickum S, Friedl P *et al.* (2007) Impaired induction of adhesion molecule expression in immortalized endothelial cells leads to functional defects in dynamic interactions with lymphocytes. *J Invest Dermatol* 127:2253–8

Orlowski RZ, Kuhn DJ (2008) Proteasome inhibitors in cancer therapy: lessons from the first decade. *Clin Cancer Res* 14:1649–57

Paramore A, Frantz S (2003) Bortezomib. *Nat Rev Drug Discov* 2:611–2

Payne AS, Cornelius LA (2002) The role of chemokines in melanoma tumor growth and metastasis. *J Invest Dermatol* 118:915–22

Perkins ND (2007) Integrating cell-signalling pathways with NF-κB and IKK functions. *Nat Rev Cell Biol* 8:49–56

Schön M, Wienrich BG, Kneitz S *et al.* (2008) KINK-1, a novel small-molecule inhibitor of IKKbeta, and the susceptibility of melanoma cells to antitumoral treatment. *J Natl Cancer Inst* 100:862–75

Shumway SD, Miyamoto S (2004) A mechanistic insight into a proteasome-independent constitutive inhibitor kappaBalpha (IkappaBalpha) degradation and nuclear factor kappaB (NF-kappaB) activation pathway in WEHI-231 B-cells. *Biochem J* 380:173–80

Soengas MS, Lowe SW (2003) Apoptosis and melanoma chemoresistance. *Oncogene* 22:3138–51

Ueda Y, Richmond A (2006) NF-kappaB activation in melanoma. *Pigment Cell Res* 19:112–24

Wang CY, Cusack JC Jr, Liu R *et al.* (1999) Control of inducible chemoresistance: enhanced anti-tumor therapy through increased apoptosis by inhibition of NF-kappaB. *Nat Med* 5:412–7

Wang JC (1996) DNA topoisomerases. *Annu Rev Biochem* 65: 635–92

Yang J, Richmond A (2001) Constitutive IkappaB kinase activity correlates with nuclear factor-kappaB activation in human melanoma cells. *Cancer Res* 61:4901–9